ACS APPLIED MATERIALS & INTERFACES

Research Article

www.acsami.org

Effect of Cooling Condition on Chemical Vapor Deposition Synthesis of Graphene on Copper Catalyst

Dong Soo Choi,[†,‡,§] Keun Soo Kim,[†,∥] Hyeongkeun Kim,[§] Yena Kim,[‡,§] TaeYoung Kim,[⊥] Se-hyun Rhy,[#] Cheol-Min Yang,[○] Dae Ho Yoon,*[,‡,▽] and Woo Seok Yang*[,§]

[‡]School of Advanced Materials Science and Engineering, Sungkyunkwan University, Suwon 440-746, Republic of Korea

[§]Electronic Materials and Device Research Center, Korea Electronics Technology Institute, Seongnam 463-816, Republic of Korea

[∥]Department of Physics and Graphene Research Institute, Sejong University, Seoul 143-747, Republic of Korea

[⊥]Department of Bionanotechnology, Gachon University, Seongnam 461-701, Republic of Korea

[#]Intelligent Mechatronics Research Center, Korea Electronics Technology Institute, Puchon 420-140, Republic of Korea

[○]Institute of Advanced Composite Materials, Korea Institute of Science and Technology (KIST), Wanju-gun, Jeollabuk-do 565-905, Republic of Korea

[▽]SKKU Advanced Institute of Nanotechnology (SAINT), Sungkyunkwan University, Suwon 440-746, Republic of Korea

Supporting Information

ABSTRACT: Here, we show that chemical vapor deposition growth of graphene on copper foil is strongly affected by the cooling conditions. Variation of cooling conditions such as cooling rate and hydrocarbon concentration in the cooling step has yielded graphene islands with different sizes, density of nuclei, and growth rates. The nucleation site density on Cu substrate is greatly reduced when the fast cooling condition was applied, while continuing methane flow during the cooling step also influences the nucleation and growth rate. Raman spectra indicate that the graphene synthesized under fast cooling condition and methane flow on cool-down exhibit superior quality of graphene. Further studies suggest that careful control of the cooling rate and CH_4 gas flow on the cooling step yield a high quality of graphene.

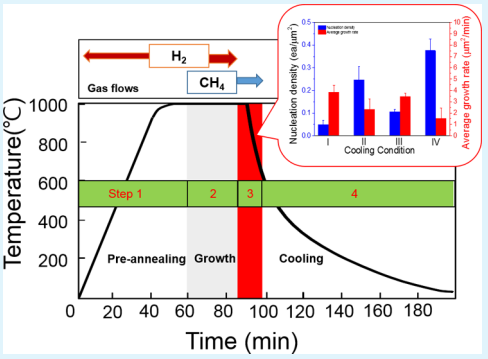

KEYWORDS: *CVD, graphene, growth, cooling rate, grain*

1. INTRODUCTION

Graphene, a two-dimensional hexagonal lattice of sp^2-bonded carbon atoms, has attracted great attention because of its prominent physical properties. High transmittance, excellent mobility, and good flexibility[1−5] have made it a promising candidate for a wide range of applications including transparent electrode in flexible electronics.[5−7]

Various methods such as mechanical exfoliation, thermal decomposition of SiC and chemical vapor deposition (CVD). Among these methods, the CVD synthesis of graphene is considered as a bottom-up method to obtain large-area graphene films with the controlled thickness.[8−10] However, CVD-derived graphene is polycrystalline with the limited grain sizes and grain boundaries composed of aperiodic heptagon-pentagon pairs or overlapped bilayer. The grain boundaries in CVD-grown graphene could degrade the mechanical and electrical properties as compared to the exfoliated graphene.[11−13] Hence, it is critically important to develop methods of controlling the grain sizes and grain boundaries, and thus improve the quality of polycrystalline CVD graphene for the practical applications including electronics.[10−14]

Recent studies of graphene growth on Ni and Cu substrates have triggered interests in understanding fundamental growth mechanism and optimizing CVD conditions for high quality graphene films. Previous reports have shown to make graphene grains with spatial structures by varying the growth parameters such as growth temperature, chamber pressure, and H_2 to CH_4 (or Ar to H_2) ratios.[11,13−15] It has been proposed that the CVD growth of graphene on Ni substrate relies on the carbon segregation and precipitation process.[16] Therefore, different segregation behavior can be produced by different cooling rates and hydrocarbon concentration retained in the CVD chamber during the cooling step. For example, a fast cooling rate is required to suppress the formation of multiple graphene layers and thus yield thin film of graphene. However, the growth on Cu substrates is due to a surface nucleation and growth process.[10,13] Therefore, variation of cooling conditions such as cooling rate and hydrocarbon concentration on the sample cooling is expected to induce different nucleation and growth

Received: June 11, 2014
Accepted: October 16, 2014
Published: November 11, 2014

behavior, affecting the overall quality of the resulting graphene films.

Herein, we describe the effects of the cooling condition on the Cu-based CVD-derived graphene synthesis. It was found that the variation of the cooling conditions such as cooling rate and methane gas flow during cooling step leads to a drastic change in the growth pattern and quality of the graphene.

2. EXPERIMENTAL SECTION

Graphene synthesis was done using a chemical vapor deposition (CVD) method as illustrated in Figure 1. Cu foil (thickness = 0.35 mm, Nippon Mining & Metals Corporation) was used as a catalyst and put into a 1.5 in. quartz tube. The quartz tube was then placed inside a 4-in. quartz tube of the CVD chamber. Ten sccm (standard cubic centimeter per minute) of H_2 was introduced to the CVD chamber, and the temperature was brought up to 1000 °C in 40 min. The Cu foil was annealed at 1000 °C for 20 min under hydrogen atmosphere of 8×10^{-2} Torr to remove copper oxide layer. H_2, CH_4, and Ar were then introduced in order into the chamber at a gas flow rate of 10, 15, and 30 sccm, respectively.

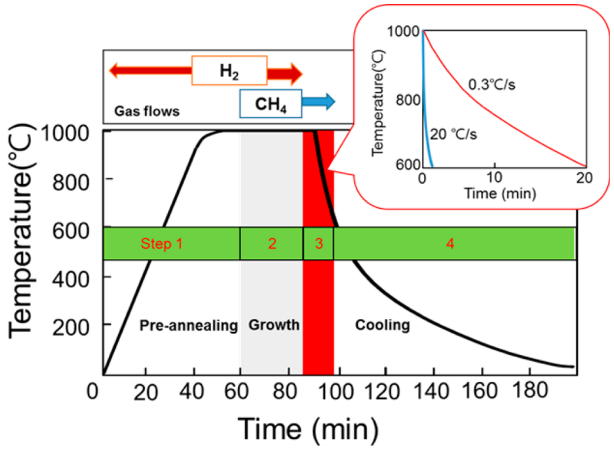

Figure 1. Conditions for graphene synthesis by chemical vapor deposition. Preannealing under hydrogen atmosphere (step 1), graphene growth under a gas mixture of hydrogen and methane (step 2), cooling under 4 different conditions to the critical temperature (step 3), and cooling to room temperature under argon atmosphere (step 4).

The graphene growth was done for 1 and 25 min under the pressure at 2.2×10^{-1} Torr. The CVD chamber was cooled to room temperature with different cooling conditions. As summarized in Table 1, four different cooling conditions were used. The fast (20 °C/s) or slow (0.3 °C/s) cooling rate were used either with CH_4 flow continuing or discontinuing.

H_2 was discontinued during the cooling steps to rule out the role of H_2. Under conditions I and II (in Table 1), the graphene samples were cooled without the continuing supply of CH_4 at fast (20 °C/s) and slow (0.3 °C/s) cooling rate, respectively, named sample 1 and 2. Under the conditions III and IV, graphenes were cooled at fast and slow cooling rates with CH_4 continuing until the temperature reaches 600 °C, which were named sample 3 and 4.

Table 1. Cooling Conditions Used in This Study

sample	cooling rate (°C/s)	CH_4 flow rate on cooling (sccm)	cooling condition
1	20	0	I (fast cooling, no CH_4 flowing)
2	0.3	0	II (slow cooling, no CH_4)
3	20	15	III (fast cooling, CH_4 flowing)
4	0.3	15	IV (slow cooling, CH_4 flowing)

For transfer process, the graphene grown on copper foil was supported by polydimethylsiloxane (PDMS) as a protective layer.[7,17] Then, the underlying Cu foil was etched away with ammonium persulfate solution (16 g of $(NH_4)_2S_2O_8$ powder dissolved in 1 L of DI water) and rinsed several times in DI water. The PDMS-supported graphene was transferred to SiO_2 (300 nm)/Si substrates and PDMS residues on top of graphene were removed by washing with acetone and isopropyl alcohol. The obtained graphene was heat-treated in a vacuum (10^{-3} Torr) at 300 °C for 10 min prior to characterization. The graphene were imaged using a field emission scanning electron microscope (FE-SEM; JSM 7500F). The electronic structure of graphene films was evaluated by Raman spectroscopy (Renishaw spectrometer, λ = 514 nm). The G and 2D peak positions and full width at half-maximum (fwhm) were determined by Lorentzian fitting[11,18,19] of the line shape of the peaks. The data in the plot for the intensity ratios and the fwhm were the average of five measurements taken from five different points. For electron transport measurement, we transferred the as-grown graphene onto Si substrates with 300 nm thermal oxide as the gate dielectric and fabricated back-gated graphene field-effect transistor (FET). Au were deposited as source and drain electrodes by thermal evaporator. The electrical properties were measured in a probe station under vacuum (3×10^{-3} Torr) at room temperature and the $I-V$ data were collected by a Keithley 4200 parameter analyzer.

3. RESULTS AND DISCUSSION

The evolution of graphene on Cu foil was monitored by varying the parameters such as the cooling rate and the CH_4 flow rate upon cooling. Four different conditions were used and summarized in Table 1. In these four processes, the annealing step under H_2, growth temperature (1000 °C), gas flow rates ($H_2/CH_4/Ar$ = 10/15/30 sccm), and chamber pressure were identical, but the cooling rates and CH_4 flowing on cooling step differed. Figure 2 shows the scanning electron microscope (SEM) images of graphene grown for 1 min under the different conditions. Rectangular or hexagonal graphene islands with mostly irregular edges were found in different areas. It is clear that average size and density of the nucleated graphene are strongly dependent on the synthetic conditions. When fast cooling conditions was used (sample 1 and 3), the density of graphene nuclei was estimated to be in the range of 0.048–0.105 ea/μm^2, which is much lower than those grown under slow cooling conditions (sample 2 and 4). The growth rate of graphene nuclei (defined here as the average area of graphene grain for 1 min) was estimated to be 3.5–3.8 μm^2/min in sample 1, 3 (condition I, III, fast cooling rate) and 1.5–2.3 μm^2/min in sample 2, 4 (condition II, IV, slow cooling rate).

In CVD growth of graphene on Cu substrate, the nuclei of graphene are initially formed and continually grow larger via a surface nucleation and growth pathway. Therefore, the average size, density and growth rate of graphene nuclei is mainly determined by the growth time, temperature, gas flow rates, and pressure, but is likely to be independent of the cooling rate.[11,13,14] However, our results show that the different cooling rates induce a change in both the density of nuclei and growth rate. For example, the nucleation of graphene occurs to a greater extent under slow cooling condition. This is likely because the slow cooling (0.3 °C/min) allows for the extended reaction time in which the CH_4 gas retained in the CVD chamber is catalytically decomposed on the Cu surface to create new graphene islands. Therefore, the density of graphene nuclei

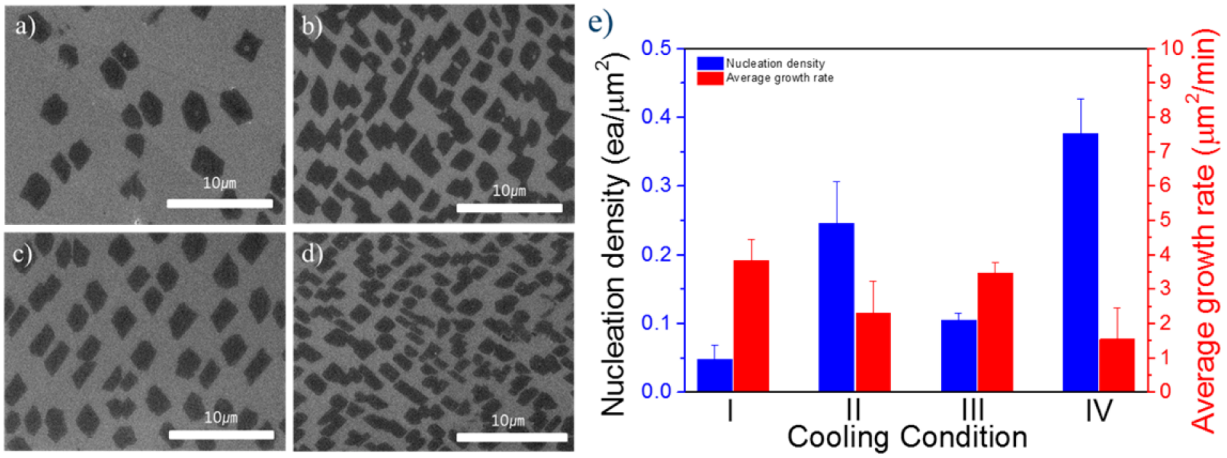

Figure 2. Graphene grown for 1 min under a gas mixture of hydrogen and methane by CVD method on sample cooling, (a) fast cooling (20 °C/s), (b) slow cooling (0.3 °C/s) under Ar atmosphere without H_2 and CH_4 to 600 °C, (c) fast cooling (20 °C/s), and (d) slow cooling (0.3 °C/s) with CH_4 continuing during cooling step. (e) Comparison of the nucleation site density and growth rate of graphene grown under four different cooling conditions.

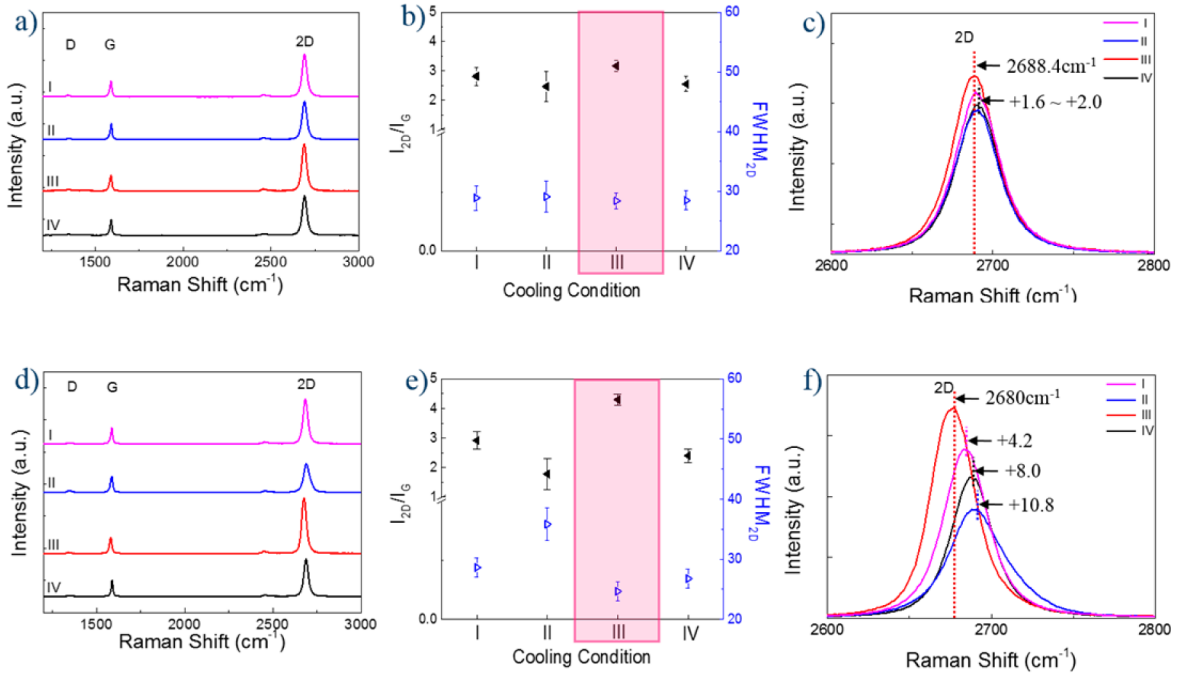

Figure 3. Raman spectra of graphene grown for 1 min (a–c) and 25 min (d–f) under different cooling condition. (a, d) Raman spectra (b, e) intensity ratio of 2D to G and fwhm of the 2D peak, and (c, f) 2D peak normalizing[25] to the G peak intensity.

was increased by decreasing cooling rate. However, the growth rate is found to be slower for the graphene (sample 2 and 4) which was grown under slow cooling rate. This could be associated with a decrease in the number of catalytic sites as the density of graphene nuclei increases and the nucleated graphene fills the Cu surface with large coverage. Therefore, the catalytic sites available for the graphene growth are somewhat limited leading to a slower growth rate. The sample 1 and 3 (fast cooling rate) showed lower density of graphene islands and relatively higher growth rate, and therefore are expected to increase grain sizes of graphene films as compared to sample 2 and 4 (slow cooling rate).

To further study the correlation between the graphene growth and cooling condition, CH_4 gas flow rate differs with 0 sccm (sample 1, 2) and 15 sccm (sample 3, 4) during cooling steps. Although the irregularly shaped graphene islands are found similarly, the density of graphene nuclei changes with respect to whether CH_4 gases were supplied during the cooling steps. The samples grown under continuing CH_4 flow on cool-down showed an increase in the density of graphene nuclei. This indicates that CH_4 gases supplied during the cooling step can chemisorb on Cu surface to form active carbon species and subsequently contribute to the nucleation of graphene irrespective of cooling rate. It is noted that H_2 gases were discontinued on the sample cooling, however as it is known that H_2 can etch carbonaceous materials not only during growth but also sample cooling, H_2 gases retained in the CVD chambers could influence the graphene growth kinetics as well.[12,18] The growth of graphene nuclei and the ultimate grain sizes of graphene grown in the presence of the remaining H_2

dx.doi.org/10.1021/am503698h | ACS Appl. Mater. Interfaces 2014, 6, 19574–19578

gases correspond to equilibrium between the graphene growth and etching. In case of continuing supply of CH_4 gases on the sample cooling, the residual H_2 gases can be swept away such that the nucleation and growth on cool-down is preferred over etching.

Raman analysis of graphene was performed to compare the qualities of the graphene samples grown under different cooling conditions and transferred to SiO_2 (300 nm)/Si substrate by PDMS similar to the reported method.[7,17] Figure 3a shows the Raman spectra collected from the center of graphene islands grown for 1 min. Two pronounced peaks in the spectrum are the G peak at ~1589 cm^{-1} and 2D peaks at ~2,689 cm^{-1}. The D peak at ~1,350 cm^{-1} is negligible confirming the presence of few sp^3–bonded carbon atoms or defects. For all of the samples, the I_{2D}/I_G intensity ratio was ~3 and the full width at half-maximum (fwhm) of the 2D peak was ~29 cm^{-1}, which represent a monolayer graphene.[10,19−27] Although all graphene samples show similar Raman spectra, the sample 3 exhibits highest I_{2D}/I_G intensity ratio and smallest fwhm value of the 2D peak (Figure 3b). In addition, the 2D peak in the spectrum of sample 3 is slightly red-shifted as compared to the other samples (Supporting Information S1).

These trends are more pronounced for the fully grown graphene samples. Figure 3d shows the Raman spectra of graphene grown for 25 min under different cooling conditions. In Figure 3e, sample 3 (fast cooling rate, CH_4 gas flow on the sample cooling) was found to have the highest I_{2D}/I_G intensity ratios and smallest fwhm of the 2D peak, indicating higher quality of the graphene. The 2D peak of sample 3 is also red-shifted as compared to the other samples (Figure 3f). Since the 2D peak position is associated with a doping concentration,[28] this result indicates that the sample is close to a pristine graphene.[25−27]

On the basis of the Raman spectra, the sample 3 that was grown under fast cooling rate with CH_4 gas flowing on the sample cooling showed the highest quality of graphene and thus was expected to have larger grain size.

The grain sizes and grain boundaries of graphene is of importance in device application since they may affect the transport properties of graphene such as the carrier mobility. The electrical properties of graphene samples grown under different conditions were evaluated with back-gated field-effect transistor (FET) devices (Figure 4).

For the device characterization, the graphene samples were transferred to the Si/SiO_2 wafer and their electron transport properties were tested at room temperature in vacuum.[29] All the devices show strong p-type doping behavior, probably because of the small volatile molecules (e.g., H_2O) physisorbed on the graphene surface during the sample processing. For the device made with graphene sample 3, the estimated carrier (hole) mobility was ~2200 $cm^2\ V^{-1}\ s^{-1}$, which is relatively high as compared to other samples (Supporting Information S2). This result suggest that better quality of graphene is derived using the fast cooling rate and methane flowing on the cool-down, which is consistent with the results from Raman analysis.

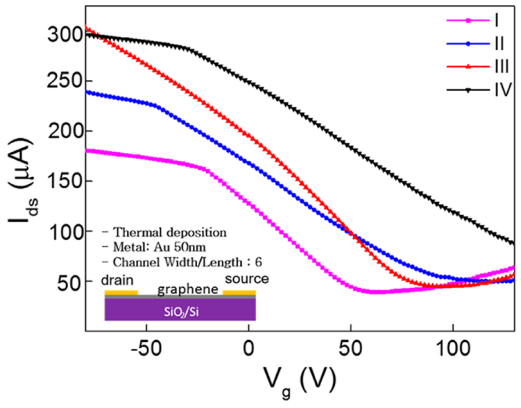

Figure 4. Transfer characteristic of the graphene back-gate FET on four different cooling conditions.

4. CONCLUSIONS

In summary, CVD growth of graphene on Cu foils under different cooling conditions has yielded islands with different sizes, density of nuclei, and growth rates. SEM images have shown that the density of graphene nuclei decreased and the growth rate increased as the fast cooling condition was applied. In addition, continuing methane flow during the sample cooling also influence the nucleation and growth of graphene on copper foil. Raman spectra indicate that the graphene synthesized under fast cooling condition and methane flow on cool-down shows the highest quality among the samples examined in this study. Further studies suggested that careful control of the cooling rate and CH_4 gas flow on the cooling step may yield a high quality of graphene.

■ ASSOCIATED CONTENT

Supporting Information

G and 2D peak positions in Raman spectra, in the case of graphene synthesized for 1 min-growth on four different cooling conditions and in the case of fully covered graphene synthesized for 25 min-growth, and the calculated carrier mobility of graphene back-gate FETs on four different cooling conditions. This material is available free of charge via the Internet at http://pubs.acs.org.

■ AUTHOR INFORMATION

Corresponding Authors

*E-mail: dhyoon@skku.edu.
*E-mail: wsyang@keti.re.kr.

Author Contributions

†D.S.C. and K.S.K. contributed equally.

Notes

The authors declare no competing financial interest.

■ ACKNOWLEDGMENTS

This work was supported by the Technology Innovation Program (No. 10044410, Commercialization of flexible touch panels based on 900 × 1600 mm^2 large, less than 1-nm thick graphene film synthesis technique) funded by the Korea Government Ministry of Knowledge Economy, Nano-Convergence Foundation (www.nanotech2020.org) funded by the Ministry of Science, ICT and Future Planning (MSIP, Korea) & the Ministry of Trade, Industry and Energy (MOTIE, Korea) (Development of Flexible/Thin Thermal Spreader Films (1,500 W/m·K, in-plane) based on solution & low temperature processes), Basic Science Research Program through the National Research Foundation of Korea (NRF) funded by the Ministry of Education, Science and Technology (NRF-2013R1A2A2A01010027), Energy Efficiency & Resources of the Korea Institute of Energy Technology Evaluation and Planning (KETEP) grant funded by the Korea Government

Ministry of Knowledge Economy (No. 20122010100130), and Korea Institute of Science and Technology (KIST) institutional program. K.S. Kim was supported by the Basic Science Research Program through the National Research Foundation of Korea (NRF) funded by the Ministry of Education (2010-0020207), Nano-Material Technology Development Program through the National Research Foundation of Korea (NRF) funded by the Ministry of Science, ICT and Future Planning (2012M3A7B4049888) and TJ Park Science Fellowship of POSCO TJ Park Foundation.

REFERENCES

(1) Nair, R. R.; Blake, P.; Grigorenko, A. N.; Novoselov, K. S.; Booth, T. J.; Stauber, T.; Peres, N. M. R.; Geim, A. K. Fine Structure Constant Defines Visual Transparency of Graphene. *Science* **2008**, *320*, 1308.

(2) Boltin, K. I.; Sikes, K. J.; Jiang, Z.; Klima, M.; Fudenberg, G.; Hone, J.; Kim, P.; Stormer, H. L. Ultrahigh Electron Mobility in Suspended Graphene. *Solid State Commun.* **2008**, *146*, 351−355.

(3) Novoselov, K. S.; Geim, A. K.; Morozov, S. V.; Jiang, D.; Zhang, Y.; Dubonos, S. V.; Grigorieva, I. V.; Firsov, A. A. Electric Field Effect in Atomically Thin Carbon Films. *Science* **2004**, *306*, 666−669.

(4) Geim, A. K.; Novoselov, K. S. The Rise of Graphene. *Nat. Mater.* **2007**, *6*, 183−191.

(5) Kim, D. H.; Ahn, J. H.; Choi, W. M.; Kim, H. S.; Kim, T. H.; Song, J.; Huang, Y. Y.; Liu, Z.; Lu, C.; Rogers, J. A. Stretchable and Foldable Silicon Integrated Circuits. *Science* **2008**, *320*, 507−511.

(6) Sekitani, T.; Noguchi, Y.; Hata, K.; Fukushima, T.; Aida, T.; Someya, T. A Rubberlike Stretchable Active Matrix Using Elastic Conductors. *Science* **2008**, *321*, 1468−1472.

(7) Kim, K. S.; Zhao, Y.; Jang, H.; Lee, S. Y.; Kim, J. M.; Kim, K. S.; Ahn, J. H.; Kim, P.; Choi, J. Y.; Hong, B. H. Large-Scale Pattern Growth of Graphene Films for Stretchable Transparent Electrodes. *Nature* **2009**, *457*, 706−710.

(8) Bae, S.; Kim, H.; Lee, Y.; Xu, X.; Park, J.-S.; Zheng, Y.; Balakrishnan, J.; Lei, T.; Song, Y. I.; Kim, Y.-J.; Kim, K. S.; Ozyilmaz, B.; Ahn, J.-H.; Hong, B. H.; Lijima, S. Roll-to-Roll Production of 30-in. Graphene Films for Transparent Electrodes. *Nat. Nanotechnol.* **2010**, *5*, 574−578.

(9) Kobayashi, T.; Bando, M.; Kimura, N.; Shimizu, K.; Kadono, K.; Umezu, N.; Miyahara, K.; Hayazaki, S.; Nagai, S.; Mizuguchi, Y.; Murakami, Y.; Hobara, D. Production of a 100-m-long High-Quality Graphene Transparent Conductive Film by Roll-to-Roll Chemical Vapor Deposition and Transfer Process. *Appl. Phys. Lett.* **2013**, *102*, No. 023112.

(10) Li, X.; Cai, W.; An, J.; Kim, S.; Nah, J.; Yang, D.; Piner, R.; Velamakanni, A.; Jung, I.; Tutuc, E.; Banerjee, S. K.; Colombo, L.; Ruoff, R. S. Large-area Synthesis of High Quality and Uniform Graphene Films on Copper Foils. *Science* **2009**, *324*, 1312−1314.

(11) Regmi, M.; Chisholm, M. F.; Eres, G. The Effect of Growth Parameters on The Intrinsic Properties of Large-area Single Layer Graphene Grown by Chemical Vapor Deposition on Cu. *Carbon* **2012**, *50*, 134−141.

(12) Vlassiuok, I.; Regmi, M.; Fulvio, P.; Dai, S.; Datskos, P.; Eres, G.; Smirnov, S. Role of Hydrogen in Chemical Vapor Deposition Growth of Large Single Crystal Graphene. *ACS Nano* **2011**, *5*, 6069−6076.

(13) Liu, W.; Li, H.; Xu, C.; Khatami, Y.; Banergee, K. Synthesis of High-quality Monolayer and Bilayer Graphene on Copper using Chemical Vapor Deposition. *Carbon* **2011**, *49*, 4122−4130.

(14) Bhaviripudi, S.; Jia, X.; Dresselhaus, M. S.; Kong, J. Role of Kinetic Factors in Chemical Vapor Deposition Synthesis of Uniform Large Area Graphene using Copper Catalyst. *Nano Lett.* **2010**, *10*, 4128−4133.

(15) Weatherup, R. S.; Bayer, B. C.; Blume, R.; Cucati, C.; Baehtz, C.; Schlogl, R.; Hofmann, S. In Situ Characterization of Alloy Catalysts for Low-Temperature Graphene Growth. *Nano Lett.* **2011**, *11*, 4154−4160.

(16) Yu, Q.; Lian, J.; Siriponglert, S.; Li, H.; Chen, Y. P.; Pei, S. S. Graphene Segregated on Ni Surfaces and Transferred to Insulators. *Appl. Phys. Lett.* **2008**, *93*, No. 113103.

(17) Yang, P.; Wirnsberger, G.; Huang, H. C.; Cordero, S. R.; McGehee, M. D.; Scott, B.; Deng, T.; Whitesides, G. M.; Chmelka, B. F.; Buratto, S. K.; Stucky, G. D. Mirrorless Lasing from Mesostructured Waveguides Patterned by Soft Lithography. *Science* **2000**, *287*, 465−467.

(18) Zhang, Y.; Li, Z.; Kim, P.; Zhang, L.; Zhou, C. Anisotropic Hydrogen Etching of Chemical Vapor Deposited Graphene. *ACS Nano* **2012**, *6*, 126−132.

(19) Reina, A.; Jia, X.; Ho, J.; Nezich, D.; Son, H.; Bulovic, V.; Dresselhaus, M. S.; Kong, J. Large Area, Few-Layer Graphene Films on Arbitrary Substrates by Chemical Vapor Deposition. *Nano Lett.* **2009**, *9*, 30−35.

(20) Wang, Y. Y.; Ni, Z. H.; Yu, T.; Shen, Z. X.; Wang, H. M.; Wu, Y. H.; Chen, W.; Wee, A. T. S. Raman Studies of Monolayer Graphene: The Substrate Effect. *J. Phys. Chem. C* **2008**, *112*, 10637−10640.

(21) Malard, L. M.; Pimenta, M. A.; Dresselhaus, G.; Dresselhaus, M. S. Raman Spectroscopy in Graphene. *Phys. Rep.* **2009**, *473*, 51−87.

(22) Lee, S.; Lee, K.; Zhong, Z. Wafer Scale Homogeneous Bilayer Graphene Films by Chemical Vapor Deposition. *Nano Lett.* **2010**, *10*, 4702−4707.

(23) Ferrari, A. C.; Robertson, J. Interpretation of Raman Spectra of Disordered and Amorphous Carbon. *Phys. Rev. B* **2000**, *61*, 14095−14107.

(24) Pimenta, M. A.; Dresselhaus, G.; Dresselhaus, M. S.; Cancado, L. G.; Jorio, A.; Saito, R. Studying Disorder in Graphite-based System by Raman Spectroscopy. *Phys. Chem. Chem. Phys.* **2007**, *9*, 1276−1291.

(25) Ferrari, A. C.; Meyer, J. C.; Scardaci, V.; Casiraghi, C.; Lazzeri, M.; Mauri, F.; Piscanec, S.; Jiang, D.; Novoselov, K. S.; Roth, S.; Geim, A. K. Raman Spectrum of Graphene and Graphene Layers. *Phys. Rev. Lett.* **2006**, *97*, No. 187401.

(26) Gupa, A.; Chen, G.; Joshi, P.; Tadigadapa, S.; Eklund, P. C. Raman Scattering from High-Frequency Phonons in Supported *n*-Graphene Layer Films. *Nano Lett.* **2006**, *6*, 2667−2673.

(27) Graf, D.; Molitor, F.; Ensslin, K.; Stampfer, C.; Jungen, A.; Hierold, C.; Wirtz, L. Spatially Resolved Raman Spectroscopy of Single- and Few-Layer Graphene. *Nano Lett.* **2007**, *7*, 238−242.

(28) Ferrari, A. C. Raman Spectroscopy of Graphene and Graphite: Disorder, Electron-Phonon Coupling, Doping and Nonadiabatic Effects. *Solid State Commun.* **2007**, *143*, 47−57.

(29) Park, J.-U.; Nam, S.; Lee, M.-S.; Lieber, C. M. Synthesis of Monolithic Graphene−Graphite Integrated Electronics. *Nat. Mater.* **2012**, *11*, 120−125.